A Review on Synthesis, Properties and Biomedical Applications of Akermanite (Suatu Ulasan Sintesis, Sifat dan Aplikasi Bioperubatan Akermanite)

Nur Hasnidah Ahmad Shukeri $^{\mbox{\tiny l.*}}$, Syed Nuzul Fadzli Syed Adam $^{\mbox{\tiny l.}}$, Hasmaliza Mohamad $^{\mbox{\tiny 2}}$ Heah Cheng Yong $^{\mbox{\tiny l.}}$

¹Faculty of Mechanical Engineering and Technology, Universiti Malaysia Perlis (UniMAP), 02600 Ulu Pauh, Perlis, Malaysia

²School of Materials and Mineral Resources Engineering, Universiti Sains Malaysia (USM), 14300 Nibong Tebal, Pulau Pinang, Malaysia

Received: 20 February 2025/Accepted: 30 July 2025

ABSTRACT

Akermanite is a bioactive calcium silicate ceramic that recently has drawn large attention and interest in biomedical devices by numerous researchers due to its favorable properties and characteristics because of the prominent element contents in this material which are Ca²⁺, Mg²⁺, and Si⁴⁺. The properties of akermanite have been studied through size particle, phase analysis, structure morphology, spectra analysis, and thermal analysis. Besides, the mechanical strength and biological properties of the akermanite also has been investigated in order to control the intended properties complied with the proper reactions of the living organism in the human body. However, despite the huge interest in akermanite in biomedical applications, a very restricted knowledge on the akermanite overview regarding its behavior and potentials are hardly to be acquired to the best of our abilities. Therefore, this review is to highlight and discuss the properties of akermanite formed upon the various methods of synthesis and various processing parameters applied and its feasible potentials in a broad range of biomedical devices practices.

Keywords: Akermanite; bioceramic; biomedical application; precursor; synthesis

ABSTRAK

Akermanite ialah seramik kalsium silikat bioaktif yang kini mendapat perhatian dan minat yang besar dalam peranti bioperubatan oleh ramai penyelidik disebabkan oleh sifat dan cirinya yang menguntungkan daripada kandungan unsur utama dalam bahan ini, iaitu Ca²+, Mg²+ dan Si⁴+. Sifat akermanite telah dikaji melalui analisis saiz zarah, fasa, morfologi struktur, spektrum dan analisis haba. Selain itu, kekuatan mekanikal dan sifat biologi akermanite juga telah dikaji untuk memastikan sifat yang diinginkan menunjukkan reaksi yang sesuai dalam tubuh manusia. Namun, walaupun terdapat minat yang tinggi terhadap akermanite dalam aplikasi bioperubatan, pengetahuan mengenai tingkah laku dan potensinya masih sangat terhad. Oleh itu, ulasan ini bertujuan untuk mengetengahkan dan membincangkan sifat akermanite yang terbentuk melalui pelbagai kaedah sintesis dan parameter pemprosesan yang digunakan serta potensinya dalam pelbagai aplikasi peranti bioperubatan.

Kata kunci: Akermanite; aplikasi bioperubatan; bahan awal; bioseramik; sintesis

INTRODUCTION

In the present climate, the medical industries are looking forward to more advancement in medical devices development alongside the enhancement in the knowledge of science and technology. This industry is currently demanding for an alternative of raw materials, processing method and the effect of the additives for the maximum impacts in the operative treatment, particularly in orthopedic clinical. The high needs in this treatment are due to the continuous defect or malfunction of bone that occurs by aging, chronic disease and traumatic bones. Besides, the bone damages can also happen due to the crucial accident which leads to deficiency in delivering the treatment

such as in bone transplant suitability, inflammatory transmission risk and immunization response system (Mohammadi et al. 2018). In addition, an issue in slow tissue recovery may also arise among the elderly that are able to provide rich bone tissue for the tissue regeneration by themselves because of osteoporosis (Mohammadi et al. 2021b). Thus, scientists and researchers are striving to create advancement and endeavor in the biomedical field concerning bone tissue engineering applications. Bone tissue engineering applications by numerous bioactive ceramic materials has produced many effective medical devices over the last decades where the admiring materials are involving hydroxyapatite, calcium silicates, glass

ceramics, magnesium silicates and magnesium-calcium silicates (Harrati et al. 2022). Even though polymeric materials has become very important biomaterials in recent years due to lower in cost and more simple processing routes, bioceramics are still preferable in specific biomedical application caused by several factors such as similarity of the mineral phase with actual bone, capability to form direct bonding between the foreign material with the host tissue and diversity of chemical composition that promotes the amendment in the mechanical properties, physicochemical properties, biocompatibility, bioactivity and biodegradability (Harrati et al. 2022; Mohammadi et al. 2021b).

Akermanite is a significant bioceramic group which categorized in an alkaline-based melilite mineral that is associated with sorosilicate class with the chemical formula of Ca₂MgSi₂O₂ (Mohammadi et al. 2021a; Myat-Htun et al. 2021; Tavangarian, Zolko & Davami 2021) and based on the CaO-MgO-SiO, system. The akermanite production in biomedical fields is growing rapidly in order to fulfill the high demands, particularly for orthopedic treatments. The production of akermanite is essential as the substitute materials in the clinical practices due to its feasible potentials that should be maximized effectively. Generally, akermanite has promises with greater degradation rate and mechanical strength compared to hydroxyapatite (HA), β-tricalcium phosphate (β-TCP) and bioglass (Mohammadi et al. 2021a; Myat-Htun et al. 2021) while capable to reach on a par with other bioceramics where it possesses with good bioactivity and osteogenic behavior that contribute the bone cells proliferation, bone forming and repair functions (Ma et al. 2019). The akermanite that consist outstanding elements where the Ca²⁺, Mg²⁺, and Si⁴⁺ ions is the main leading as it is in charge for the essential roles for the implementation in the bone tissue engineering applications including stimulates the osteoblast growth, enhance the production of collagen, accelerates the growth of bone and controls the immunization system (Dasan et al. 2022; Tavangarian et al. 2020). Technically, calcium (Ca) is significant in the bone matrix, magnesium (Mg) acts well in the growth and repair functions of bone tissues while silicon (Si) works in the formation of bone skeletal systems respectively (Mohammadi et al. 2018). Furthermore, the release of Ca ions is also the one caused osteoblast proliferation, the Si ions support the osteogenesis and angiogenesis as well as increase the mineralization, meanwhile the Mg ions regulate the degradability of the ceramic (Tavangarian et al. 2020; Zadehnajar et al. 2021). The release of these ions has demonstrated the crucial effects on cell growths, differentiations and binding in the bone treatment (Tavangarian et al. 2020). Several techniques on synthesizing and processing of the akermanite have been studied by previous researchers in order to alter the desired properties to suit with its target applications. Due to its encouraging responses in orthopedic practices, this paper has reviewed some of the methods and precursors that can

be used for synthesizing akermanite. This discussion also includes the effect of synthesis and processing methods, precursors and temperature parameters used on several important characteristics and properties of the synthesized akermanite to see whether it is suited to be implemented in biomedical application.

SYNTHESIS ROUTE OF AKERMANITE

Synthesis of akermanite (Ca₂MgSi₂O₂) can be implemented by several techniques of synthesis including sol-gel, dry spraying, selective laser sintering and solid state method. Commonly, the productions of akermanite are engaged with sol-gel method. Nevertheless, the sol-gel normally involves higher cost for reagents and precursor materials, consumes longer processing time and requires continuous supervision during operating for a certain duration (Harrati et al. 2022; Mohammadi et al. 2021a; Tavangarian, Zolko & Davami 2021; Tavangarian et al. 2020). The sol-gel approach that involves wet methods promises to be controllable in shape and sizes precisely yet brings difficulties in adjustment of crystallinity and phase composition of nanopowders (Zadehnajar et al. 2021). The sol-gel method may also produce akermanite with high contents of carbon due to the suppressed densification happening during the sintering process (Sharafabadi et al. 2017). However, porous akermanite scaffold can be obtained by sol-gel method followed with drying, calcinations and selective laser sintering technique which produces 61.2% of porosity at 150 mm/min of scanning speed, the least among the entire data (Han et al. 2014). The production of akermanite via sol-gel method with the additive solution of ethanol and 2M nitric acid has produced lowest density with larger pores than 10 µm and lowest chemical stability compared to diopside and baghdadite that allowed for more calcium ions to release which preferable for bone scaffold applications (Najafinezhad et al. 2017).

In addition, another approach to produce akermanite powders which is a dry spraying method. There is a previous study that has differentiated various techniques between sol-gel, ball milling and spray drying methods followed with further heat treatment for the akermanite production (Duman & Bulut 2021). They have been summarized that the dry spraying method is used for coating materials and it is the most effective technique for the fine size particle distribution of akermanite fabrication with controllable shapes and compositions of the ceramic powders compared to the sol-gel and ball milling approaches (Zadehnajar et al. 2021). However, the challenges of the dry spraying method for akermanite include the additional procedures in initial particle preparation in order to provide uniform and fine particles and avoid agglomerations occurring during dry spraying. Besides, crucial considerations of nozzle equipment and processing parameters are required for the purpose of controlling the layer coating to achieve favorable porosity, density and mechanical strength of akermanite. Next, the microsized amorphous akermanite can also be prepared by the flame synthesis technique after the melt quenching process. This flame synthesis has been applied with high cooling rates in order to avoid crystallization and the production of the powders are formed at almost absolute spherical shape for the purpose of 3D scaffold manufacturing (Dasan et al. 2022). The uniform shape of the akermanite microsphere powder provides favorable outcomes for the 3D printing of scaffolds. This is because it promotes excellent viscous flow properties in additive manufacturing applications compared to conventional powders and creates a highly macroporous scaffold with numerous additional pores between particles due to incomplete densification appropriate for bone tissue applications (Dasan et al. 2021). Yet, flame synthesis is known well with complexity processes where it requires specialized equipment to maximize flame parameter processing. Furthermore, material impurities and nanoparticle agglomeration may also happen due to excessive high temperature and require additional final steps such as dispersion.

Moreover, solid states techniques are also regularly operated to develop the akermanite powder. This method is frequently applied because of its simplicity in handling, cheaper in production cost and less time consuming compared with the sol-gel method that has been mentioned previously (Mohammadi et al. 2021a; Myat-Htun et al. 2021). The synthesizing of akermanite through solid state method also promises a fine particle size of powders that promotes high thermodynamic and kinetic reactions between the precursor materials (Myat-Htun et al. 2021). Mechanical activation via high planetary ball milling is also one of the solid state methods that aims to alter the physical size of the materials into nanopowders (Mohammadi et al. 2018). This is in contrast with other studies where the milling activations are limited for large particle sizes and produce impurities in akermanite products (Zadehnajar et al. 2021). There is a study that applied wet high-speed and high-energy planetary ball milling to mix CaO, MgO, SiO, powders homogeneously with 500 rpm milling speed for 3 h (Mohammadi et al. 2018). The milled powders are dried sieved, pressed and sintered at 1200 °C with 5 °C/min for 4 h as heating rate, in results produced 45.69 nm crystallite size of akermanite with tensile strength acquired, 5.71 MPa which is within the human cancellous bone (1.5-38 MPa). Plus, a study on high-energy planetary ball milling with 500 rpm and sintering temperature at 1250 °C contributes the most dense ceramic sample as much 96.83% effectively appropriate for bone repair treatment (Myat-Htun et al. 2021). On the other study (Mohammadi et al. 2021a), the successful of akermanite formed was obtained with 13.7 MPa of diametric tensile stress and 95.4% of relative density with 1.76 µm of average particle size by high-energy ball milling and thereafter of sintering process at 1250 °C for 6 h. Besides, it has been reported that the ball milled powders of talc, calcium carbonate and silica at 500 rpm for 20 h and

subsequent 1200 °C annealing for 5 h produces akermanite tablets with 2.489 g/cm³ density, 24.7 MPa compressive strength and 3800 MPa Young's Modulus (Tavangarian et al. 2020). Therefore, it summarized that the solid state via high ball milling followed by a sintering process could be a simple and straightforward procedure for akermanite synthesizing compared to the other methods. Besides, this approach has cost effectiveness, versatility for a wide materials range, controllable properties and is capable of processing in bulk powder quantities where the outcome of the materials are high in purity with less contamination risk.

INITIAL RAW PRECURSOR FOR AKERMANITE

Due to the plus points exhibited by the akermanite for the biomedical device applications, there are multiple precursors that can be used in processing the akermanite bioceramic that has been implemented by previous study. Ideally, any materials involving calcium, magnesium and silica contents are proficient enough for the akermanite formation as listed in Table 1. As the example from a study by Mohammaadi et al. (2021a, 2018), the mixture of CaO, MgO and SiO, powders with stoichiometric ratio of akermanite, 2:1:2, respectively, were wet ball milled with milling speed of 500 rpm, dried, pressed and sintered at 1200 °C for 4 h, has successfully produced nanoparticle powders of akermanite ceramics with 45.69 nm of crystallite size and admirable diametric tensile strength within the range of human cancellous bone. The outstanding formations of apatite layer on the surface of the samples were observed by Field-Emission Scanning Electron Microscopy (FESEM) analysis once the samples were soaked into the SBF solution for 7 days also indicating the favorable biological performances of produced akermanite.

Similarly with a study by Myat-Htun et al. (2021) that produced akermanite by using CaO, MgO, and SiO, powders with molar ratio of 2:1:2, respectively, via wet ball milling and sintering with vary processing parameters on the milling speeds and sintering temperatures. They stated that the higher milling speeds could provide better structure for akermanite leading to preferable properties of the ceramics that support them as promising candidates for bone regeneration applications. They also concluded that the optimum sintering temperature above 1100 °C mostly showed single phase of akermanite while the formation of multiple phase compounds such as low clinoenstatite, wollastonite, monticellite, and diopside occurred at low temperatures below 700 °C due to unstable structure and incomplete crystallization. The formation of akermanite has confirmed to achieve the highest value of the diametrical tensile strength of akermanite samples compared to previous researches at 1200 °C which is able to reach the amount about 32.10 ± 2.13 MPa which excessively greater than the recorded values of other prominent bioceramics such as pseudo-wollastonite, CaSiO, (5.04 MPa), HA (4 MPa) and β-TCP (2.85 MPa) besides considerably

TABLE 1. Summary of varying akermanite synthesis by different precursors, sintering parameters and its outcomes

	Sint	erino n	Sintering parameters		Mochania			
Precursors	Temp.	Time (h)	Heating rate (°C/min)	Crystallite size (nm)	strength (MPa)	Morphology	Bioactivity performances	References
20.56 g CaO, 7.39 g MgO, 22.03 g SiO ₂	1250	9	8	1760	$\sigma_t = 13.70$	The relative density of the microstructure can obviously be seen where porosities are nearly diminished	NR	(Mohammadi et al. 2021a)
2:1:2 ratio of CaO, MgO, SiO ₂	1250	8	10	45.5	$\sigma_{\rm t} = 32.10$	Grain growths with well-defined grain boundaries were observed and prone to attach to each other and form larger grains. The larger grains are surrounded with small grains which occupy the voids and enhance the density	NR	(Myat-Htun et al. 2021)
2:1:2 ratio of CaO, MgO, SiO ₂	1200	4	v	45.69	$\sigma_{\rm r} = 5.71$	The grain microstructures of the akermanite were even and uniformly distributed but did not clearly present its grain boundaries after the sintering process	Obvious apatite layer forms after 7 days of SBF immersion. Value of pH achieved within 7.69-7.72 after 28 days, which is in the range of human biological value	(Mohammadi et al. 2018)
1:6:2 ratio of talc, CaCO ₃ , SiO ₂	1200	ς.	10	35	$\sigma_{_{\rm t}}=24.70$	The surface structures of the akermanite illustrated rough and irregular surfaces with non-uniform grain growth. The morphology showed high porosity on the structure which may enhance the bioactivity properties	The apatite layer was gradually formed until 28 days of immersion. Concentration of Ca, Mg and Si ions increased while P ions decreased with the increasing duration of SBF immersion (28 days). Optimum pH achieved after 2nd days of immersion (7.9)	(Tavangarian, Zolko & Davami 2021; Tavangarian et al. 2020)
$2:1:2$ ratio of egg shell, MgO, SiO_2	006	κ	W	500	$\sigma_{c} = 210$	Large amounts of microporous structures were observed on the akermanite with a neatly uniform pore size distribution (0.5-10 µm) which was able to support the cell growth and bioactivity	Micropores reduced after 28th days of immersion due to hydroxyapatite layer formation. Pure akermanite has higher apatite formation compared to multiphase akermanite (associated with merwinite + diopside)	(Sharafabadi et al. 2017)
Dolomite & pearlite	1250	7	6	NR	$\sigma_b = 7.71$ $\sigma_t = 3.56$	Agglomerations of the grains were increased, leading to the increasing densifications and elimination of porosities on the surface of the sintered material	Apatite formation gradually increased until 28 days and entirely filled the voids in samples where the density increases. Maximum pH reached after 5 days immersion (7.56) and remained stable until 21 days	(Harrati et al. 2022)
Dolomite & slag 1200 waste	1200	7	v	NR	$\sigma_{t}=13.80$	The particles are bonded together forming large grains and the size of porosities is reduced, subsequently creating dense sintered ceramic	NR	(Arkame et al. 2023)

*Denoted that the σ_i indicates diametrical tensile strength, σ_e is compressive strength and σ_{bend} is bending strength. Meanwhile, NR indicates data are not recorded by the study

higher than the value of the current cancellous human bone which is at the range of 1.5-38 MPa. Meanwhile, the micro hardness of akermanite milled at 500 rpm and sintered at 1250 °C was about 4.94 \pm 0.26 GPa greater than the natural bone due to high density and low porosity of the akermanite.

Another study from Tavangarian, Zolko and Davami (2021) and Tavangarian et al. (2020) has used the mixed powders with molar ratio of 1:6:2 of talc (as Mg and Si source), calcium carbonate and silicate with 500 rpm milling speed and subsequent annealing at 1000 °C for an hour. The findings on the fine crystallite size of akermanite samples around 21-28 nm were obtained which reached the correlation with the morphology of akermanite samples by Scanning Electron Microscopy (SEM) analysis that showed micro porous surfaces. On the other hand, Sharafabadi et al. (2017) also has utilized natural waste such as eggshells as Ca sources associated with MgO and SiO, powders as the initial materials for the akermanite production. The eggshells were heat treated at 100 °C for 2 h to eliminate the undesired protein contents. The heat treated eggshells were mixed together with other initial materials via planetary ball mill for 6 h at 400 rpm with stoichiometric ratio and sintered at 900 °C at different sintering durations. Although the sintering process is only at 900 °C is which considerably low sintering temperatures compared to other studies, it has been recorded that the akermanite phase has reached its fully crystallite and diminished the merwinite phase after 3 h of sintering. Besides, many micropores were observed uniformly on the akermanite structures with size distribution about 0.5-10 µm where the pores were filled completely by apatite formation after 28 days of SBF immersion. The compressive strength of akermanite that sintered for 3 h also has reached approximately 210 ± 7 MPa which surpassed the compressive strength of hydroxyapatite. The compressive strength could be improved with higher sintering time (5 h) up to 240 ± 8 MPa but restricts the bioactivity of the akermanite considering the low apatite formation after the SBF immersion due to the low porosity structures that hinders the dissolution properties of akermanite.

Moreover, the production of akermanite can also be developed by natural mineral resources such as dolomite which is acquired from sedimentary rock minerals called as dolostone. The dolomite material contains high constituents of calcium and magnesium contents with minor impurities such as Si, Al, Na, C, K, Mn, Cu, Ti, and Fe which has been reported by several studies (Mustafa et al. 2016; Shahraki, Mehrabi & Dabiri 2009; Tursunov, Dobrowolski & Nowak 2015). The calcium from dolomite is capable of playing a vital role in maintaining and enhancing the strength and structure of human bone. Meanwhile, the magnesium promotes the bone metabolism and mineralization of the bone tissues with rapid proliferation rate (Arokiasamy et al. 2022). Additionally, both of these elements are able to present solid antibacterial activity due

to the existence of oxides compounds (Yamamoto et al. 2008) that proven the favorable biological performances of dolomite and encouraged this mineral to participate in the applications for bone tissue engineering. Besides, the natural characteristics of dolomite as a pore-former agent are also capable of contributing for the formation of porous bone scaffold that leads to the development of bone tissue regeneration and instant recovery process (Cai et al. 2021; Ren et al. 2019). Therefore, researchers have gained more interest to study the potential of dolomite material for the production of akermanite due to the abundance of this mineral with controllable properties that are suitable for biomedical purposes.

A study by Arkame et al. (2023) where the Moroccan dolomite mineral was utilized along with slag waste from the steel industry and formed the akermanite phases associated with merwinite and diopside in the prepared samples which are promising for biomedical potentials. The addition of slag at the range of 0-30% into the dolomite is for the reason of improving the mechanical strength and providing low thermal conductivity. These powders were milled and sieved at 50 µm particle size and subsequently pressed, dried at 105 °C for 24 h and sintered with double-step. Initially, the compacted powder samples were sintered at 600 °C for 2 h to allow the decomposition of carbonates to happen and then subsequent sintering at higher temperatures were executed around 1100-1300 °C for next 2 h. The findings quoted the optimum properties obtained at 1200 °C with 50.28-41.4% porosity, 1.7-1.89 g/cm³ density, 28.07-24.8% water absorption, and 1.55-6.25% shrinkage by increasing the addition of slag. The recorded mechanical strength of the produced samples is 13.8 MPa with 30% of slag and considered acceptable due to the presence of zero micro cracks on the surface of the samples by SEM analysis.

Furthermore, the utilization of Moroccan geomaterials involving dolomite and natural pearlite for the production of akermanite bioceramic also showed great favorable properties which were provided in a study by Harrati et al. (2022). The high sintering at 1250 °C with 3 °C/min heating rate towards the mixtures from both of these raw materials have successfully formed prominent akermanite phases in the ceramic samples with slightly presence of diopside and periclase despite the differences in mixture compositions within 0-30% of natural pearlite addition. The akermanite sample from 75:25 wt. % composition of dolomite to pearlite has reported to create the most favorable ceramic sample compared to other prepared mixtures with 43.84% porosity, 25.43% water absorption, 1.78 g/cm³ apparent density and bearable bending and tensile strengths upon high loads with the values of 7.71 MPa and 3.56 MPa, respectively. The linear and volumetric shrinkage owned by this ratio mixture sample also found out to be the lowest values compared to the results obtained by other mixture samples which is 2% and 5.92% individually. Moreover, this akermanite sample has produced great surface

morphology with the absence of any damages, defects or cracks on the surfaces and instead an obvious formation of apatite layer has completely covered the surface of the samples which reserves for an excellent result for *in-vitro* analysis that could be exhibited for the applications in biomedical field.

Overall, these studies prove that the dolomite can be used as the superior precursor for akermanite production. The ideal composition of dolomite with rich contents of Ca and Mg can contribute vital roles in bone regeneration by providing the sufficient sources of calcium and magnesium based. Although dolomite commonly has other elements as the impurities substances, it does not involve any hazardous compounds and safe for biocompatibility applications which supported this mineral to be used as biomaterials. The small amount of impurities usually does not raise any noticeable impact but it still can be diminished by the heat treatment process if required. Thus, it is encouraging to study the potential of Perlis dolomite as the raw material for akermanite bioceramic particularly for biomedical device practices. This is because abundance of local dolomite is easily acquired in nature with low cost consumption compared to other specialized raw materials. However, dolomite main applications especially in Malaysia are currently limited to constructions and agriculture industries, not in biomedical applications (Che Azurahanim et al. 2022; Hussin et al. 2006; Nazry et al. 2006). To the best of our studies, there is a deficiency of scientific data that has been made on Malaysian dolomite as the raw material in the preparation of akermanite bioceramic. Due to the promising properties and behavior of this mineral resource, the utilization of Malaysian dolomite should be explored concerning akermanite production in order to enhance their mineral value and induce a new alternative of bioceramic material for practical uses in the biomedical industry.

TEMPERATURE FOR AKERMANITE FORMATION

The DTA and TGA are used to examine the thermal properties that occur during the calcination process in order to support the decomposition of the akermanite synthesize. By referring to DTA curves, it has been recorded that the formation of akermanite does not exist at low sintering temperature below 500 °C due to the absence of exothermic or endothermic peaks on the spectra (Sharafabadi et al. 2017). This can be supported by another studies where the milled powders of CaO, MgO, and SiO, that has been sintered presents the thermal properties as shown in Figure 1 where three endothermic peaks are obtained at 396, 440, and 718 °C indicated the formation of enstatite, diopside and merwinite phase, respectively, while an exothermic peak is seen at 881 °C attributed as akermanite crystallite (Myat-Htun et al. 2021). Similarly, the DSC curves have illustrated the minor endothermic peak at 640 °C and an exothermic peak at 840 °C which showed the decomposition of calcium carbonates and akermanite phase respectively (Tavangarian, Zolko & Davami 2021).

They also reported two stages of weight loss of the ceramic samples that can be observed by TGA curves which initiate from 300-560 °C and 560-675 °C which may be due to the moisture removal and decomposition of carbonates. Besides, Harrati et al. (2022) has stated that the synthesis of dolomite and perlite would induce the presence phases of wollastonite (CaSiO₃) and enstatite (MgSiO₃) at 900 °C, merwinite (Ca₂SiO₄) at 1000 °C and lastly akermanite (Ca₂MgSi₂O₇) and diopside (CaMgSi₂O₆) at 1250 °C as in the Equations of 1-5.

$$CaO + SiO_2 \rightarrow CaSiO_3$$
 at 900 °C (1)

$$MgO + SiO_2 \rightarrow MgSiO_3$$
 at 900 °C (2)

$$CaO + CaSiO_3 \rightarrow Ca_2SiO_4$$
 at 1000 °C (3)

$$2 \text{ Ca}_3 \text{Mg}(\text{SiO}_4)_2 + \text{MgSiO}_3 + \text{SiO}_2$$
 at $1250 \,^{\circ}\text{C}$ (4) $\rightarrow 3 \text{ Ca}_3 \text{MgSi}_3 \text{O}_7$

$$CaSiO_3 + MgSiO_3 => CaMgSi_2O_6$$
 at 1250 °C (5)

PROPERTIES OF AKERMANITE

Physical, Chemical & Mechanical Properties of Akermanite In terms of physical properties, akermanite material is able to resist high temperature as its melting point is above 1450°C with theoretical density of 2.944 g/cm³ (Mohammadi et al. 2021a; Wu & Chang 2004). A study has recorded that the akermanite processed from precursors of CaO, MgO and SiO, powders via wet high-energy ball mill and sintering process at 1200 °C created 0.93±0.25 µm of grain size, 45.69 nm of crystallite size that comes along with 63.73% of density, 35.59% of porosity and 17.30% of linear shrinkage (Mohammadi et al. 2021a). Moreover, the increasing speed of ball milling from 300-500 rpm can also produce the grain size of akermanite at the range of 45.5-43.3 nm with the specific surface area (BET) within 77.79-108.68 m²/g along with high densification from 93.72-96.83% after sintering process at 1250 °C (Myat-Htun et al. 2021). Meanwhile, there is a study that proved the increasing in the milling duration from 10 to 20 h will cause the particle size of akermanite powders to be increased within 21-28 nm as shown in Figure 2 due to the frequent frictions between the initial materials and agglomeration of nanocrystals (Tavangarian, Zolko & Davami 2021) which was approximately close with the crystallize size of akermanite powders where at the range of 20-80 nm (Tavangarian et al. 2020). They also reported that the increasing in ball milling duration causes the increasing in density of akermanite samples and decreasing in porosity as shown in Figure 3 which also leads to sample shrinkage as much as 15% for the reason that more gases escape from the tablet samples during the sintering process. Besides, grain size of the akermanite particles also could be decreased due to the increasing sintering temperature from 1200 °C to 1250 °C, which enables the increase in porosity, density as well as diameter

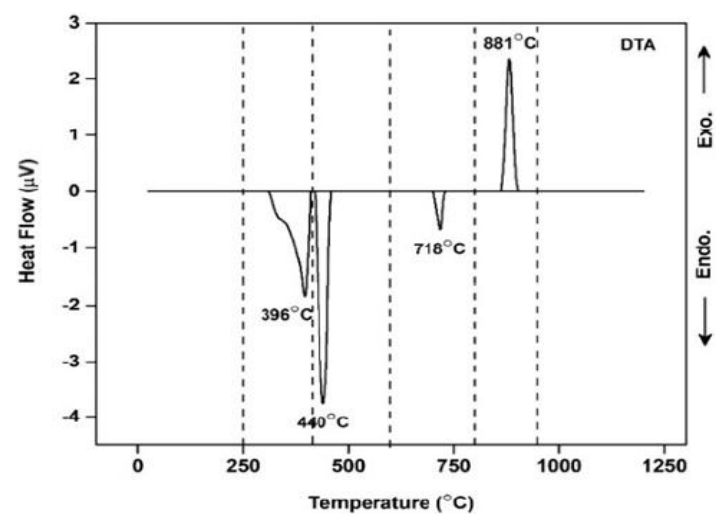


FIGURE 1. DTA curve of sintered ceramic powders at different temperatures (Myat-Htun et al. 2021)

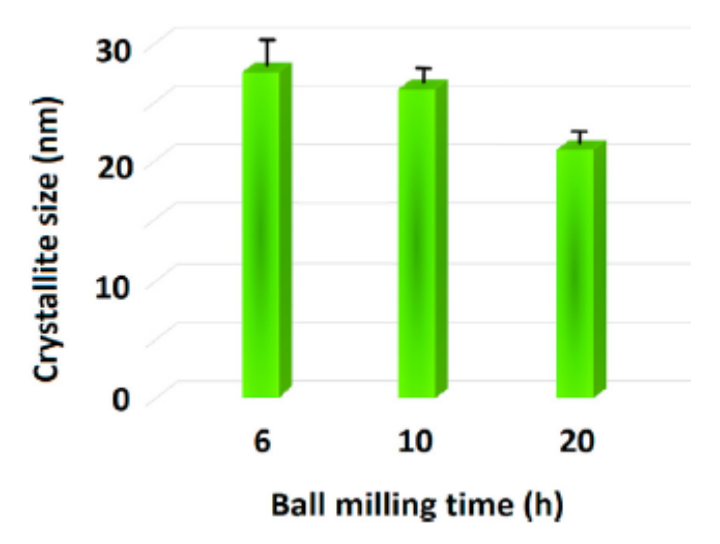


FIGURE 2. Crystallite size of akermanite powders at different ball milling times (Tavangarian, Zolko & Davami 2021)

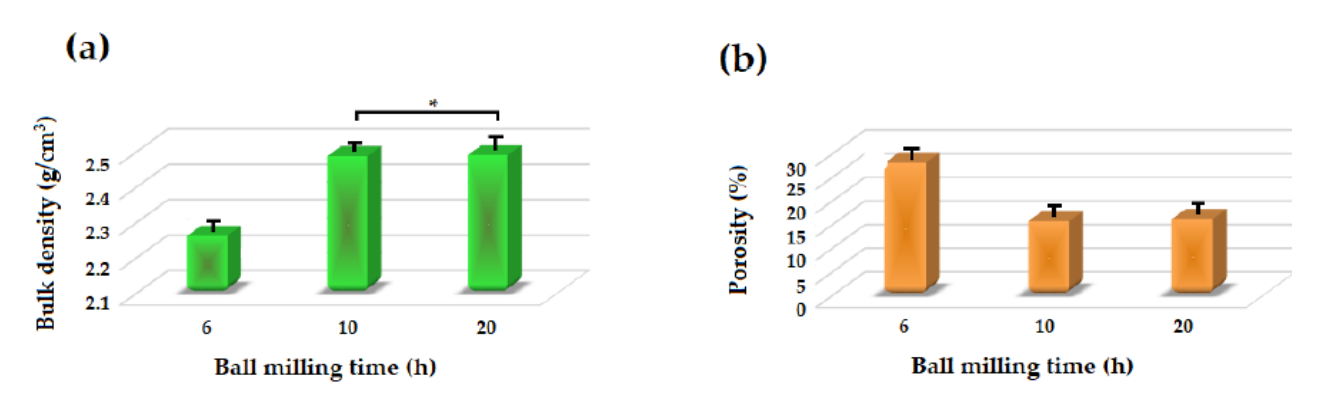


FIGURE 3. Properties of (a) bulk density and (b) porosity of akermanite samples at multiple ball milling times (* noted as slightly different values) (Tavangarian et al. 2020)

shrinkage of the akermanite samples (Mohammadi et al. 2021a). They have stated that the diffusion that happens due to the phase decompositions has allowed the pores removal which leads to low amounts of pore volume while promoting the larger grains formation and raises the densification resulting in the shrinkage to happen. Next, despite ball milling and sintering parameters, another study has reported that the akermanite developed from dolomite and 25.0 wt. % of natural perlite as additives was able to produce 43.84% porosity, 25.43% water absorption, 1.78 g/cm³ apparent density, 2.0% linear shrinkage and 5.92% volume shrinkage (Harrati et al. 2022).

Regarding the mechanical properties, the compressive strength, tensile strength, hardness and toughness of the akermanite were discussed to determine the potential of akermanite in biomedical applications especially for bone implant applications. In general, the mechanical strength of the akermanite can be directly influenced by the physical and chemical properties that occur in the samples due to the type of synthesis process. The diametric tensile strength of akermanite samples able to reach about 32.10 ± 2.13 MPa (Myat-Htun et al. 2021) which are mainly higher than other bioceramics such as HA (4 MPa) and β-TCPA (2.85 MPa) as well as considerably greater than normal cancellous human bone (1.5-38 MPa) (Mohammadi et al. 2021a, 2018) which contributes this akermanite material preferable as bone grafting substances. Besides, the increasing ball milling speed up to 500 rpm also improved the microhardness of akermanite samples about 4.94 ± 0.26 GPa and 1.62 ± 0.02 MPa.m^{1/2} of fracture toughness due to the denser akermanite sample produced from milled nanopowders (Myat-Htun et al. 2021). According to Harrati et al. (2022), the increasing of densification and reduction of porosity of the akermanite samples promotes the rises in the flexural and tensile strength from 3.34 to 8.66 MPa and from 1.81 to 4.31 MPa, respectively, due to the addition of perlite (0-30%) in the dolomite mixtures. The compressive strength of 5 h sintering time also increased approximately at 240 ± 8 MPa which is higher than the values obtained by 3 h sintering time which is nearly at 210 ± 7 MPa because of the reduction of porosity (Sharafabadi et al. 2017). They also recorded that the compressive strength of the samples are decreased once the soaking process of the samples leads to the release of oxide ions into the SBF solution which is similar with other studies (Díaz-Pérez et al. 2021). Next, the compressive strength of the akermanite can also be influenced by the lattice structure of the 3D scaffold design. It has recorded that the Kagome structure is an apparent lattice almost adequate for the bone treatments that may involve bearable loads as the compressive strength obtained is around 28 MPa in the nitrogen atmosphere which lower than cubic (6 MPa) and diamond lattice structure (24 MPa) (Dasan et al. 2022) which also undefeatable with the small values obtained for the exact structures from other study (Dasan et al. 2020).

Structure and Phase of Akermanite

Theoretically, the crystal structure of akermanite is tetragonal as in Figure 4 that has been classified in the similar space group of 113 which is P42₁m (Mohammadi et al. 2018; Yang et al. 1997), formed by MgO₄ tetrahedral plane with Si₂O₇ groups and crosslink together with large cations of Ca (Sharma 2022).

According to the analysis on XRD, the findings on akermanite formation from dolomite and pearlite materials has shown the phase transformation (Figure 5) which dominantly by akermanite phases followed with subordinated phases of diopside, periclase and merwinite upon the addition of pearlite from 0-30 wt. % (Harrati et al. 2022). These phases were found similar as in other reported studies indicating the findings are consistent and support the validity of current results (Myat-Htun et al. 2021). They also have recorded that the formation of akermanite and diopside phases were found in major while the periclase and merwinite phases were decreased in the ceramic mixtures within 22.5 wt. % and 27.5 wt. % of pearlite. In addition, a fully crystallite of akermanite phases that neatly match with the standard pattern of JCPD 01-087-0047 also were created while merwinite phases were removed from the samples during the calcination powders at 900 °C for 3 h (Sharafabadi et al. 2017). Besides, the pure akermanite phases were also observed in another study without any impurity such as diopside and merwinite once the calcination at 1200 °C (Najafinezhad et al. 2017) while at 1300 °C (Wu & Chang 2004) via sol-gel techniques where the most prominent diffracted peak of the akermanite phase exists roughly at the 2 theta = 31° . Even though the increasing sintering temperature has shown phases transformation on the ceramic samples shown by multiple researchers, there is another study presented definite contrast where no changes on the diffracted peaks between unsintered and sintered samples, showing that the presence of neither new phases nor transformation had happened with relatively matching patterns with the standard PDF data of JCPD 83-1815 (Han et al. 2014).

Based on the observation of FTIR findings, it has been confirmed that the phase transformation of akermanite does not completed yet at low sintering temperature (500 °C and 700 °C) indicated by the absence bands of O-Ca-O and Ca=O in the spectra (Sharafabadi et al. 2017). Meanwhile, the segregation of broadening bands was noticed at 900 °C indicating the existence of whole characteristic functional groups in the akermanite samples as shown in Figure 6(c). It has been recorded that the spectrum presented bending modes of O-Ca-O at 411 cm⁻¹ and O-Mg-O at 473 cm⁻¹. The bands at 589 cm⁻¹ represent the ionic bond between calcium and oxygen ions. The bands of O-Si-O have existed at 641 cm⁻¹ and 680 cm⁻¹, the stretching modes of Si-O are at 848, 932 and 981 cm⁻¹ while the symmetric vibration mode of Si-O-Si stretching band is at 1021 cm⁻¹. All these peaks of akermanite are found available

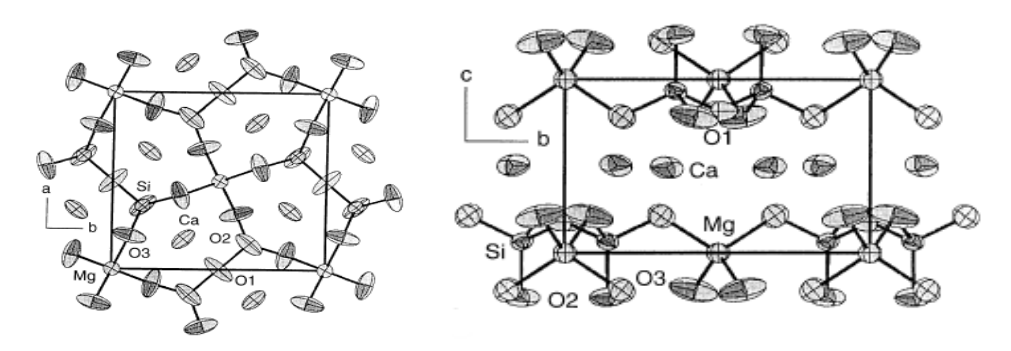


FIGURE 4. Akermanite crystal structure at room pressure (Yang et al. 1997)

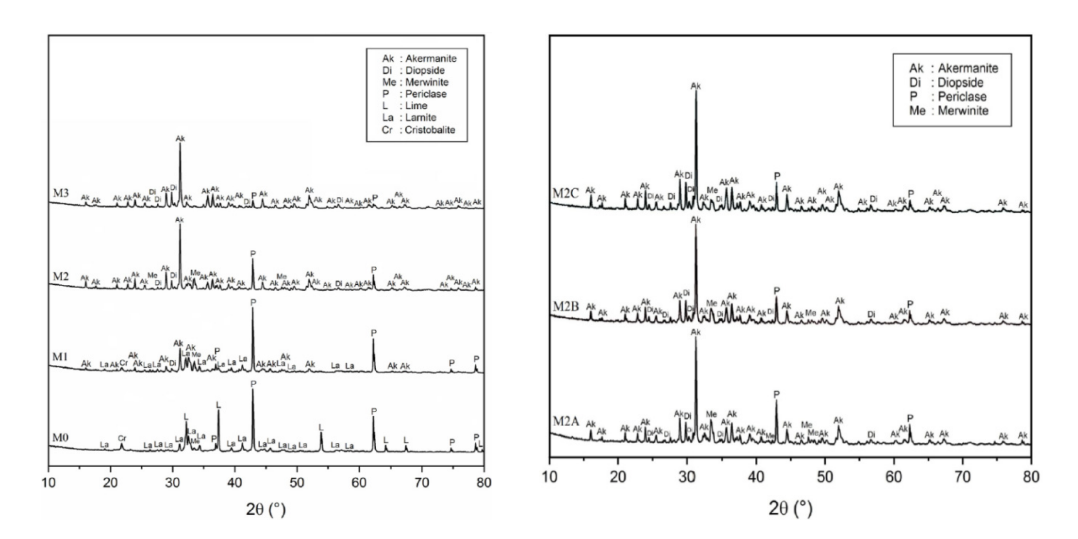


FIGURE 5. XRD spectra of ceramic samples sintered at 1250 °C for 2 h (Addition of perlite wt. % denoted as M0=0%, M1=10%, M2=20%, M2-A=22.5%, M2-B=25%, M2-C=27.5% and M3=30%) (Harrati et al. 2022)

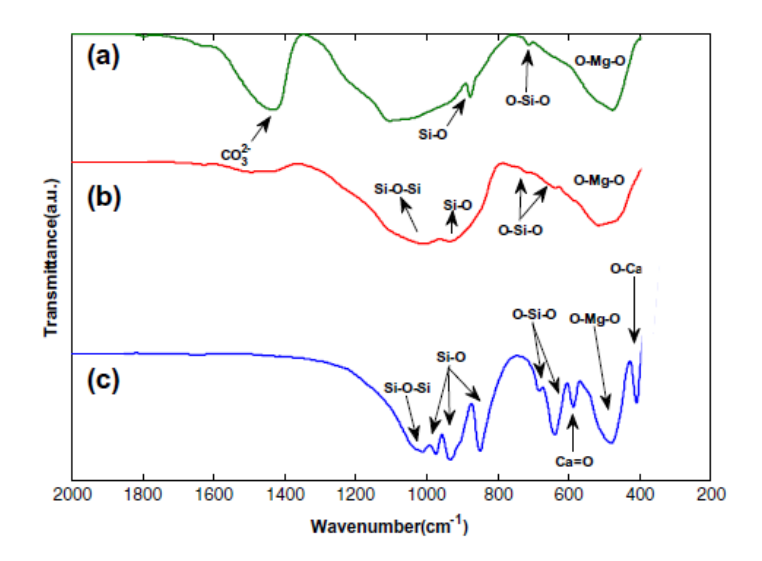


FIGURE 6. FTIR spectra of ceramic powders sintered at (a) 500 °C, (b) 700 °C and (c) 900 °C (Sharafabadi et al. 2017)

in the other reports which showed a great agreement with other studies (Mohammadi et al. 2018; Najafinezhad et al. 2017). Yet, additional peaks were found at 1646 cm⁻¹ that reserved for the bending vibration of H₂O molecules while the wide absorption peak at 3442 cm⁻¹ indicated the —OH moisture band of stretching vibration mode (Harrati et al. 2022) similarly with Choudhary, Koppala and Swamiappan (2015). Besides, Choudhary, Koppala and Swamiappan (2015) also has spotted an asymmetric stretching band at 1400 cm⁻¹ because of the separation of CO₂ from silicate bioceramic samples during the calcinations process at 1200 °C.

Morphology of Akermanite

Generally, the powder particles of akermanite were almost in round shape with numerous micro porous structures on the surface (Harrati et al. 2022; Tavangarian et al. 2020). An example of akermanite morphology was shown in Figure 7 where this akermanite was synthesized from dolomite and natural pearlite. The porous particles are agglomerated and binding together (Tavangarian et al. 2020) while creating a pore size distribution at the range of 1-10 µm once the sintering process based on the SEM scale (Harrati et al. 2022). However, it has been stated that the ideal pore size of the bioceramic scaffold for the application of bone tissue formation is in between 100 and 400 µm where the least acceptable is 100 µm, suggested pore size for bone formation is 300 µm and above while the most active in osteogenesis activity is 400 µm (Mohammadi et al. 2021b). Next, the morphology of akermanite concerning graft scaffolding also presents the similar porous structures as mentioned. Apart from the grain size and porosity of the structures, the silicone-based of akermanite scaffolds had macro cracks and minor defects within the struts which could be unnoticeable upon the addition of fillers such as anhydrous borax (Na₂B₄O₇) and homogenous blends of commercial silicones with photocurable resin as shown in Figure 8 (Dasan et al. 2020). The inappropriate selection on the anhydrous borax unfortunately contributes to the cracks generation due to the agglomeration instead of solving the ceramic transformation issues through the gas immersion. The high thermal application also is significant in the fabrication of scaffold as it promises the desirable viscous flow that determines the porous matrix and surface finish of the structure (Dasan et al. 2021, 2020). Plus, it has been concluded that the endorsement of topologies structure could be impactful to the binding phase of the struts as well as the compressive strength of the scaffold where Kagome structure is preferable than diamond and cubic structures (Dasan et al. 2022). Besides, a study has concluded that the high sintering time (6 h) and temperature (1250 °C) are also able to turn the micropores structure into a dense structure as the grain size and density increases while the porosity decreases (Mohammadi et al. 2021a).

Bioactivity of Akermanite

The bioactivity performances of the akermanite can be observed by the formation of apatite that was developed

after the soaking process into SBF for a certain period. Akermanite immersion into SBF for 28 days caused fully occupied of pores with the growth of apatite and reduced the porosity as well as devoted the desirable biological behavior on the akermanite ample which reached the agreement with another study (Sharafabadi et al. 2017). The layers of apatite that formed were fine spherical shapes where the continuous growth of the apatite are developed until 28 days of immersion as shown in Figure 9 (Harrati et al. 2022) in contrast with another study where shuttlelike of apatite were found in the scaffold of akermanite (Han et al. 2014). Generally, the apatite formation on the morphology structures indicates the in vivo and bioactive properties of the samples which can be applied for the bone tissue engineering application. Meanwhile, the EDS analysis that has been obtained by several studies has shown similar results where elements of Ca, Si, Mg and O are demonstrated in the EDS spectra which verified the dominant compositions of akermanite phases (Harrati et al. 2022; Sharafabadi et al. 2017). The presence of phosphorus peak and the increase of calcium peak relative to the reduction of magnesium and silica amount can be observed once the samples are soaked into SBF. The phosphorus element is representing the layer of apatite formed due to the bioactivity reaction between the sample and the SBF. The immersion after 28 days has reduced the intensity amount of silica and a complete elimination of magnesium from the samples as shown in Figure 10 due the apatite formation that has covered the surface of the samples entirely (Harrati et al. 2022).

APPLICATION OF AKERMANITE IN MEDICAL DEVICES

The production of akermanite has been gradually developed in the biomedical field due to its bioactivity properties. The favorable characteristics of akermanite in terms of mechanical strength and biodegradability are also able to reach or exceed the values obtained by other prominent bioceramics such as hydroxyapatite (HA) and tricalcium phosphate (TCP). Thus, the broad applications of akermanite in biomedical devices are the significant actions that could be taken in order to acquire a rapid recovery in bone tissue treatments efficiently. Table 2 summarize the reported findings regarding the influence of the precursor, processing methods and sintering parameters on the mechanical and bioactivity outcomes of the akermanite-based material, highlighting their relevance for medical applications including bone scaffold, bone implant and coating material.

Akermanite Application as Bone Scaffold

In the present time, the akermanite production has been implied for numerous applications in bone scaffolds in a par with HA and TCP in fact akermanite is highly potential than those of both bioceramics due to its impressive osteogenesis (Liu et al. 2008) that included complete set of bone cell types as illustrated in Figure 11. Besides, this statement can be supported because the HA and β -TCP

scaffold are bounded as brittle materials that leads to low mechanical strength compared to the cortical bone and causes poor toughness and easily fracture on the large load bearing area of the scaffold (Mohammadi et al. 2021b). Meanwhile, akermanite is possessed with good bioactivity, biocompatibility, controlled biodegradability and improved mechanical strength (Collin et al. 2021; Dobrita et al. 2023;

Liu et al. 2008). The favorable properties of akermanite can be altered to comply with the desired scaffold applications mainly due to the chemical composition of this bioceramic which are calcium, magnesium and silica contents (Collin et al. 2021). Ideally, the high contents of calcium in the akermanite provides the main constituent for the bone regeneration followed by magnesium and

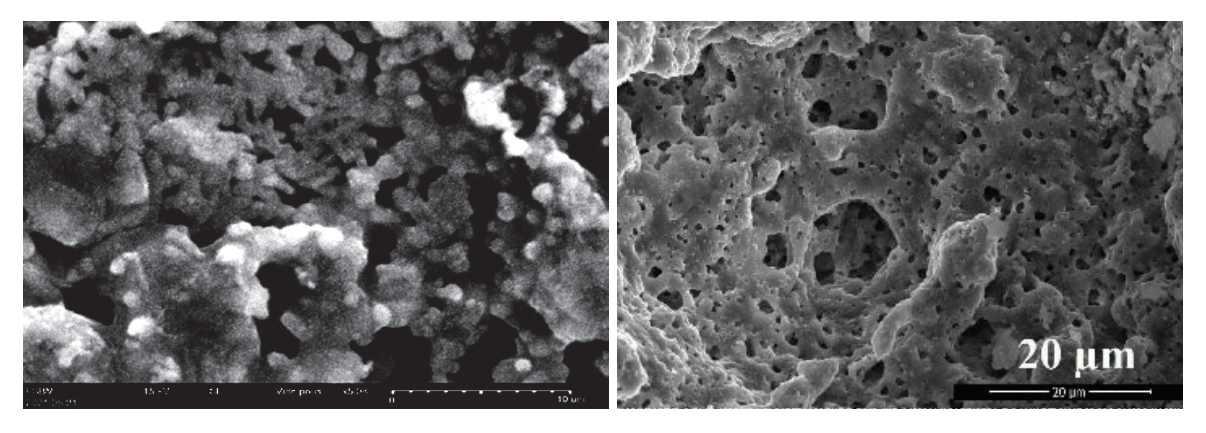


FIGURE 7. Round-shape and micro porous morphology of akermanite (Harrati et al. 2022; Tavangarian et al. 2020)

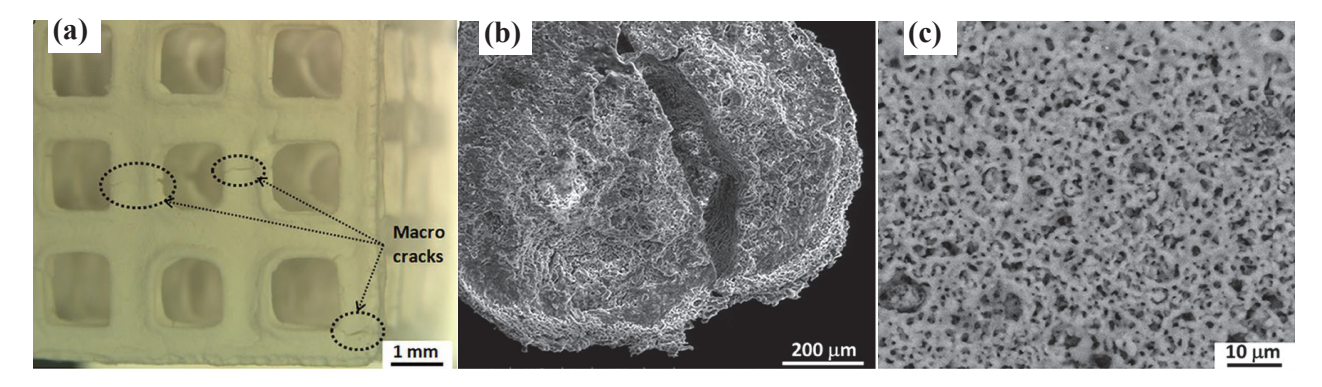


FIGURE 8. Microstructures of silicone-based of akermanite scaffolds with addition of anhydrous borax fillers and photocurable resin that had (a) macro cracks, (b) minor defects within the struts and (c) microporous structure of the struts (Dasan et al. 2020)

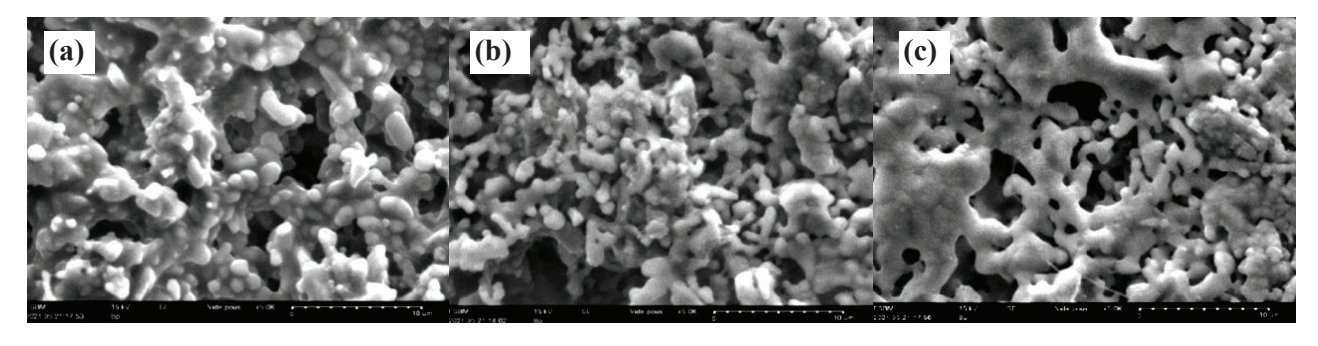


FIGURE 9. SEM analysis of akermanite, (a), (b) and (c) after soaked for 14, 21 and 28 days into SBF, respectively (Harrati et al. 2022)

TABLE 2. The impact of precursor, processing techniques and sintering parameters on the mechanical and bioactivity performances

	References	(Liu et al. 2016)	(Dobrița et al. 2023)	(Han et al. 2014)	(Duman & Bulut 2021)	(Bernardo et al. 2014)	(Youness, Zawrah & Taha 2024)	(Li, Zhang & Zhang 2024)
	Bioactivity performances	Akermanite has active mRNA expressions due to release ions that directly contact to the scaffold	Has higher cell proliferation with increasing 4% compared to the samples before immersion and it increases up to 8.6% after 3 days of immersion	An apatite layer formed after 14 days and continuously coats the entire substrate after 21 days. Lamellipodia outgrowth and cytoplasm were observed after a day indicating cell proliferation. Cell form aggregates on the 5th day and entirely covers the surface at 9th day	Smooth surface of the scaffold nearly covered entirely by the thick layer of bone-like apatite after soaked in SBF solution. The apatite formation gradually appeared on the interconnected porous area of the scaffold and formed a dense and homogeneous surface	Borax addition may not significantly affect the bioactivity performance due to inability to degrade the biocompatibility of the akermanite scaffold due to the $\mathbf{B_2O_3}$ and $\mathbf{Na_2O}$ existence	Hydroxyapatite layer can be observed in the entire prepared akermanite scaffold despite the contents of NaCl	Cell adhesion can clearly be observed on the β -TCP/AK-micronano scaffold surface. It provides active osteogenic genes in rBMSCs and elevates the degradation rate. The pH values were consistently increased along the Tris-HCl immersion
	Mechanical properties (MPa)	$\sigma_{c} = 71.2$ MPa and reduced to 14 MPa after soaked in Triss buffer	$\sigma_{_{c}}=1.90\pm0.1~\mathrm{MPa}$	$\sigma_c = 5.92 \pm 0.41 \text{ MPa}$	High content of akermanite (80 wt. %) in chitosan improves the strength up to $\sigma_c = 3.10 \text{ MPa}$	$\sigma_c = 3.4 \pm 0.2$ (no borax) $\sigma_c = 5.1 \pm 0.4$ MPa (5 wt. % of borax)	$\sigma_{c} = 138 \text{ MPa}$ $H_{V} = 3.75 \text{ GPa}$ $E = 63 \text{ GPa}$	Akermanite improves about 20% of mechanical properties compared to pure β-TCP
1	Technique	Sol-gel + 3D direct ceramic ink writing	Sol-gel + 90° orientation of 3D printing	Selective laser sintering at 150 mm/min of scanning speed	Sol gel + pneumatic 3D printing + freeze drying	AI mold + solid state sintering	Calcination + solid state sintering	Digital light processing (DLP), debinding + sintering
	Precursor	Akermanite powder	Ratio CaO:MgO:SiO ₂ of 2:1:2	Akermanite powder	Chitosan + akermanite powder	H62C polymer, $Mg(OH)_2$, $CaCO_3 + 5 wt$. % of borax	Akermanite + 15 vol. % of NaCl contents	β-TCP + Akermanite powder
	Application				Bone			

page
previous
trom
continue

(Ma et al. 2019)	(Díaz-Pérez et al. 2021)	(Liu et al. 2016)	(Yue et al. 2024)		(Zhang et al. 2023)	(Putra et al. 2023)
Akermanite extracts in the rats body does not exhibit any <i>in vivo</i> subchronic systemic toxicity and pathological changes to significant organs such as the heart, liver and kidneys which indicates its biocompatibility behavior as bone implant material	The akermanite phase was totally removed and left porous hydroxyapatite formation on the surface after SBF immersion due to faster dissolution of the akermanite phase compared to merwinite	Akermanite with high Mg-containing increases degradation rate and relative surface areas and supports more new bone regenerations, 94% and 261% higher compared to Hardystone and β-TCP. Akermanite produces higher pH and remains till 9 weeks. Intermediate layer riches with phosphorus were observed after 4 weeks of post-implantation attributed to the formation of a calcium phosphate deposition	Akermanite with 9% Mg presents fewer micropores than pure akermanite leading to faster bio-dissolution and increases the pH value after soaked in Tris buffer. 9% Mg in akermanite causes superior hone formation but noor osteogenic canacity compared	to pure akermanite although it remains increases till 120 days	Weight loss after SBF immersion does not present and measurable value for 4 weeks due to pre-allloyed raw material, high sintered density of composite and dense formation of ions on the layer Higher akermanite promotes better cell growth on the composites with well-spread morphology with spike-like filopodia anchoring the surfaces	30% of akermanite promotes higher biodegradability. Meanwhile, the value of pH remains at 7.68 which is the appropriate value for implant material. The <i>in vitro</i> findings show that the adhesion, proliferation, and osteogenic differentiation of preosteoblasts were observed and suitable for bone implant substitute fabrication
NR	$H_{\rm V} = 5.74~{\rm GPa}$ $K_{\rm IC} = 0.78~{\rm MPa\cdot m^{1/2}}$	N. R.	9 % Mg akermanite (σ_b = 16.40 MPa and σ_f = 14.71 MPa) has higher strength than pure akermanite	$(\sigma_b=13.70~MPa$ and $\sigma_f=11.95~MPa)$	50% of akermanite/ Fe35Mn creates great mechanical strength, ($\sigma_c = 403 \text{ MPa}$, $E_c = 18 \text{ GPa}$, $H_v = 228 \text{ HV}$) compared to pure Fe35Mn	Fe35Mn + 20% Akermanite presents higher mechanical properties ($\sigma_{\rm y} = 8.3$ MPa, E = 0.53 GPa) than Fe35Mn + 30% Akermanite
Injection into rats	Sintering + laser floating zone (LFZ)	Sol-gel + material implantation on ovariectomized osteoporotic rat model	Wet chemical co-precipitation + DLP 3D printing + implantation on	rabbit femoral condylar defect	Powder metallurgy + solid state sintering	Extrusion-based 3D printing + debinding + Sintering
Extracts of akermanite + saline control	$CaO, MgO, SiO_2 + PVA$	Akermanite	Mg-CSi powders		Akermanite + Fe35Mn powders	Fe + Mn + Akermanite powders
			Bone Implant			

	раде	
	previous	
	trom	
•	continue	

(Dong et al. 2021)	(Bakhsheshi- Rad et al. 2019)	(Razavi et al. 2014b)		
3D printed Electroconductive Polylactic Acid (EC-PLA) coated with 10 wt. % akermanite creates low porosity that allows nutrients and blood to pass through the open porous structures and promotes cell proliferation and osteoblast growth	PLLA-AKT coating on the Mg alloy reduces the degradation rate yet unable to hinder the spread and infiltration of bacteria causing <i>S. aureus</i> and <i>E. coli</i> . Incorporation of low DOXY with PLLA-AKT coating on MG alloy may be required in order to enhance the antibacterial performances and improve cytocompatibility	Akermanite coated on an AZ91 sample showed slow degradation rate with high cell attachment and spreading through SEM analysis indicating its great initial cytocompatibility compared to uncoated samples		
$\sigma_{c}=30~\mathrm{MPa},\mathrm{E}=40~\mathrm{MPa}$	After 7 days of SBF immersion: $\sigma_c = 237 \text{ MPa},$ $\sigma_b = 11.8 \text{ MPa}$	After 4 weeks of SBF immersion: $\sigma_c = 130 \text{ MPa}$		
3D printing and freeze-drying technology	Sol-gel + sintering + powder mixing + electrospinning	Sol-gel + Micro arc oxidation (MAO) + electrophoretic deposition (EPD)		
Chitosan + Magnetic nanaoparticles (MNPs) + Akermanite	Akermanite + poly-L-lactic acid (PLLA)	Akermanite powder		
	Coating Material			

silica elements that promotes the biodegradability rate and develops osteogenesis and angiogenesis while enhances mineralization of the implants, respectively.

A study by Liu et al. (2016) on the fabrication of bioceramic scaffolds has been implemented between akermanite and TCP formation by using conventional sol-gel techniques with subsequent procedures including 3D direct ceramic ink writing and single step of sintering process at 1100 °C for 3 h with 2 °C/min as heating rate. The entire findings have shown outstanding performances on the akermanite scaffold compared to TCP scaffold. The average porosity of both scaffolds does not exhibit significant changes which are at 53% and 56% for akermanite and β -TCP scaffold, respectively, which is assumed due to the slight differences in sample shrinkage during sintering at high temperature. Besides, it has been recorded that the akermanite scaffold has reached substantial compressive strength of 71.2 ± 6.7 MPa, which is 7 times greater than the value obtained by β -TCP scaffold (10.5±3.0 MPa). Meanwhile, the mechanical strength of the akermanite scaffold still shows relatively high values after immersion around 14 MPa compared to β-TCP scaffold and even higher than the strength of host cancellous bone which roughly within 5-10 MPa, reported by other study (Liebschner 2004). In the perspective of biological properties, the akermanite scaffold has proven active mRNA expressions of osteogenesis genes due to the released ions of Ca, Si and Mg in Tris buffer which promotes new bone tissue contact directly into the scaffold.

Meanwhile, the fabrication of porous akermanite scaffolds with CaO, MgO, and SiO, powders-based has put a concern particularly in the pattern orientation of the designed scaffold (Dobrita et al. 2023). They found out that the 3D printing of 90° orientation scaffold has higher porosity at 83.10% relatively produced lower compressive strength of 1.90 \pm 0.1 MPa due to huge ions loss during high sintering temperature at 1370 °C caused by the great interconnectivity of pores and less intersections between the struts in contrast with 3D-45° orientation scaffold. They also recorded that the 3D-90° creates higher cell proliferation with increasing 4% while 3.5% for 3D-45°, and gradually improves up to 8.6% and 4.7% respectively, after the 72 h of immersion that promises the potential in biomedical applications for bone treatment. Based on Deng et al. (2023), the acceptable degradation rate would demonstrate little impact on the akermanite samples despite the design of gradient scaffolds due to the full interconnectivity of the scaffold struts. Next, the potential in bone tissue applications by akermanite scaffold via selective laser sintering at the 150 min/min of scanning speed also has produced the optimum compressive strength of 5.92 ± 0.41 MPa with accelerated proliferation rate upon the scaffold with the increasing period (Han et al. 2014).

Next, an approach to produce excellent mechanical strength of the biomaterial combined with outstanding bioactivity performances is one of the challenges in

akermanite bioceramic scaffold. This is because favorable bioactivity normally comes from high porosity scaffolds which may lessen the mechanical properties. Therefore, a reaction between polymer-derived from anhydrous sodium borate was modified into the formulation of akermanite scaffold inks resulting in high purity of akermanite phase with minor traces of wollastonite. Besides, addition of borax has created zero crack akermanite scaffolds with dense struts with compressive strength around 7.3 ± 1.1 MPa which approximately twice higher than pure akermanite scaffolds that are still suitable for bone tissue engineering (Dasan et al. 2019). Contradiction to another study, akermanite with 5% borax has shown the optimum compressive strength at 5.1 ± 0.4 MPa with numbers of porosity, meanwhile, the akermanite with zero borax and 15% borax does not present much difference between each other in term of its porosity and mechanical strength (Bernardo et al. 2014). However, they have stated that the borax addition in akermanite may not affect the bioactivity performances because the presence of B₂O₂ and Na₂O existed in amorphous phase and could not degrade the biocompatibility of the akermanite scaffold. Moreover, Youness, Zawrah and Taha (2024) has summarized that the increasing NaCl contents (15-50 vol. %) in akermanite has demonstrated poor performances of the scaffolds whereas the least amount of NaCl (15 vol %) is the most sufficient concentration needed as it reached the most dense structure and leads to highest compressive strength of 138 MPa, microhardness at 3.75 GPa and Young's Modulus at 63 GPa. Despite that, the HA layer still can be observed in the entire prepared akermanite scaffold from 15 vol. % to 50 vol. % NaCl which has the potential to mimic native human bone structures and encourages the akermanite as promising candidates for bone scaffold implementation.

Akermanite Application as Bone Implant

Bone treatments that involve bone implant applications usually would be considered for the older patients with critical defects at high load-bearing bone areas which require immediate strength of the bones for the purpose of providing the bone functionality and get back to daily routines comfortably. Since bone implants are essential in orthopedic and dental practices, various kinds of materials have been implemented in these procedures regarding the unique properties of the materials and compliance for specific applications. Metals such as titanium alloys and stainless steels are one of the materials that are widely used for permanent bone implants due to its impressive strength, wear and corrosion resistance, yet have few challenges in metal allergies and are heavy in overall implant weight compared to other materials. On the other hand, polymers like Polylactic Acid (PLA) are synthetic materials that are lightweight and have great biodegradability behavior suitable for bone implants. However, polymers-based implants are usually not ideal and inappropriate for high load applications due to low mechanical strength

and degradation complications that affect surrounding tissues. Meanwhile, bioactive and biodegradable ceramics such as HA and TCP are commonly used due to its biocompatibility and osteoconductivity behavior that accelerates bone regeneration that is almost similar to the human bone matrix. It is often used as temporary scaffolds in bone grafting as it will degrade over time catching up with the bone tissue growth and accelerate the healing process as shown in Figure 12. Despites typical drawbacks of bioceramic which are brittleness properties, bioactive ceramics especially derived by akermanite have received rising interests for the bone implants applications.

The production of akermanite has been recognized by its positive reactions in biological performances through multiple reports regarding its toxicity, biocompatibility and immunization responses respected to be implied as bone implant. Based on a study by Ma et al. (2019), they have confirmed the biosafety of akermanite bioceramic as bone implants according to in vivo ISO standard methods where akermanite extracts were injected into rats. They reported that the akermanite extracts demonstrated no toxicity activity towards the cell tissues of the host where appropriate osteogenic bioactivities were observed with insignificant reactions on the main blood cells functions and zero disruptions on the entire important organs of the host. Ionic microenvironment by the akermanite bioceramics through Ca, Mg, and Si ions release is able to accelerate the bone regeneration and reduces the immune responses (Díaz-Pérez et al. 2021). Furthermore, another biological investigation on bone defects of the rats models was carried on by using a Mg-containing akermanite, hardyston (Har), and beta-tricalcium phosphate (β-TCP) (Liu et al. 2016). They concluded that the akermanite bioceramic has superior performances in new bone formation with increased osteoblastic activity and greater degradation proportion compared to Har and β -TCP.

Attributed to the challenges of akermanite production with excellent mechanical alongside with great bioactivity performances, addition of other substances into the akermanite based may be a percipient alternative for bone implant materials. A designed 3D porous bioceramic by 9% Mg rich contents in akermanite not only enhance the sintering property, but also has improved the mechanical strength properties where the compressive and flexural strength reach up to 16.40 ± 0.63 MPa and 14.71 ± 1.52 MPa, respectively (Yue et al. 2024). The Mg contents in the akermanite also accelerate the bone formation faster than the pure akermanite, besides, has low biodegradable rate where the materials can still be identified from the surrounding tissue even after 120 days. Moreover, a study has fabricated iron manganese alloys (Fe35Mn) associated with addition of akermanite via a powder metallurgy technique concerning orthopedic implant applications (Zhang et al. 2023). Due to slow degradation rate, poor mechanical strength and bioactivity performances, the influence of akermanite at different contents within 0-50

volume % in the Fe35Mn were investigated. The results showed the increasing contents of akermanite in Fe35Mn have improved the in vitro biocompatibility followed by human osteoblast by the formation of a rich layer of phosphate on the samples. The increasing contents of akermanite also able to enhance the value of relative density (~ 94-97%), compressive yield strength (~403 MPa), elastic modulus (~18 GPa) and microhardness (~228 HV) compared to the pure Fe35Mn. However, the ductility of the samples was decreased at higher concentration of akermanite addition which is 30% and 50%. This statement has a contradiction with another study where the addition of akermanite at 20% and 30% has reduced the yield strength and elastic modulus of the biomaterial (Putra et al. 2023). They have assumed it was due to the impacts of embrittlement by the bioceramic phase on the metal matrix. However, the results on the mechanical strength of the Fe35Mn/akermanite still meet the requirements of the human bone strength. Therefore, these findings have concluded the potential of akermanite on Fe35Mn as biodegradable material in bone implant applications.

Akermanite Application as Coating Material

Theoretically, the coating material that is used in the application of bone implant is for the purpose of optimizing the performance neither in terms of mechanical strength, magnetism, biodegradation or biocompatibility. In this study, it has been mentioned repetitively according to the utilization of bioceramic material in biomedical devices due to its unique properties. However, in some orthopedic practices, metallic and polymer are used as the materials of the implants. These materials could cause complications due to corrosion and wear rate, degradation issues as well as infection and immune responses due to the ionic environment where the elements release from the implants. Thus, the coating materials by bioceramics are applied associated with the implants to avoid excessive bonding forces during high load that may lead to great deformations and possibly to cause cracks or defects on the surface matrix and at the same time improve the biodegradability and bioactivity performances for the bone regeneration as demonstrated in Figure 13.

Based on a study by Dong et al. (2021) they have investigated the influences of akermanite percentages in the polymeric solution as the coating material on the properties of the scaffold via freeze-drying method. The addition of akermanite within 0-30% by this method aids to improve the mechanical strength and biological properties equivalent with the host tissue without any complication or harm on the living tissue. Besides, they also reported that the freeze-drying technique is able to boost threefold of the compressive strength for the magnetic scaffold. Ideally, the increasing of akermanite in the coating solution may cause the increasing in the porosity to relatively increase the compressive strength, cross linking and failure prevention of the coated scaffold. The results of 10 wt. % akermanite on

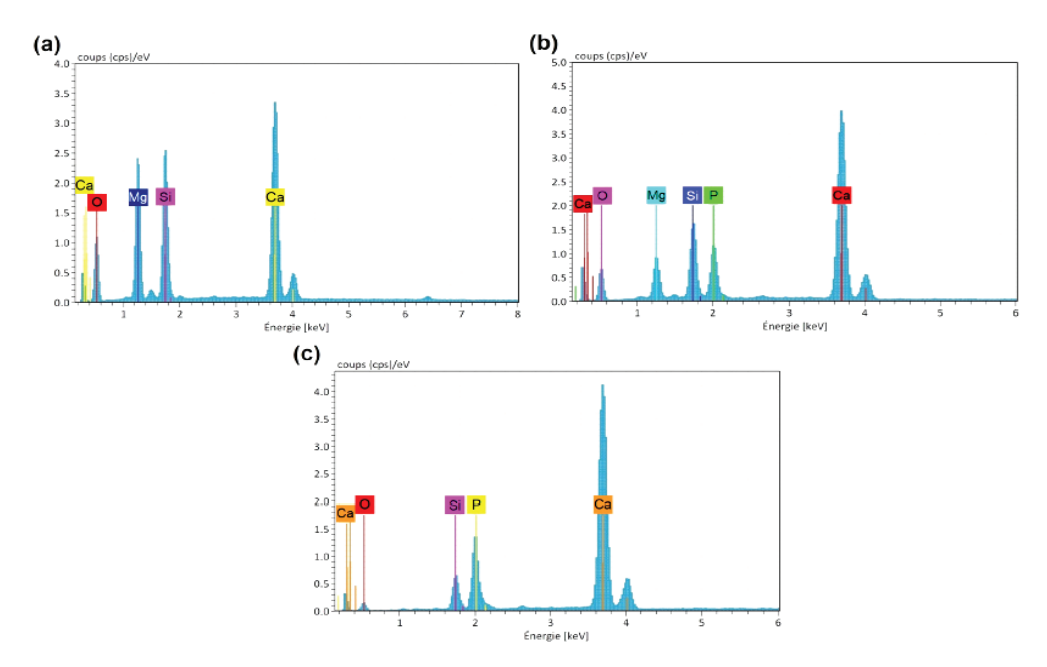


FIGURE 10. EDS analysis of akermanite, (a) before, (b) and (c) after soaked for 21 days and 28 days, respectively (Harrati et al. 2022)

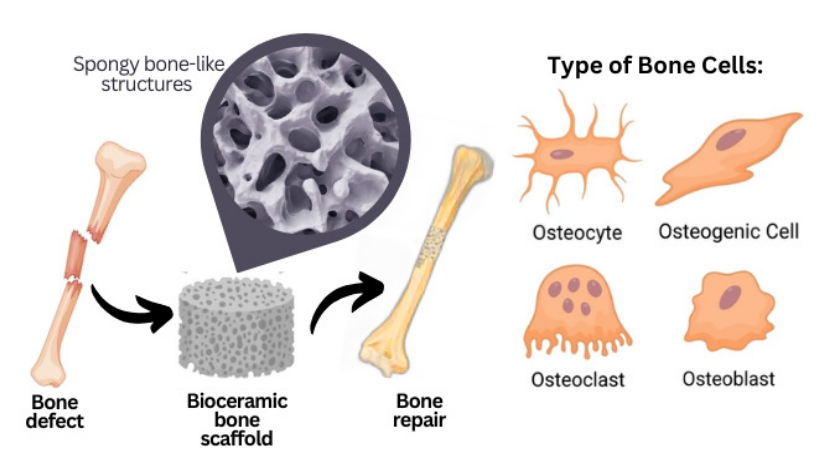
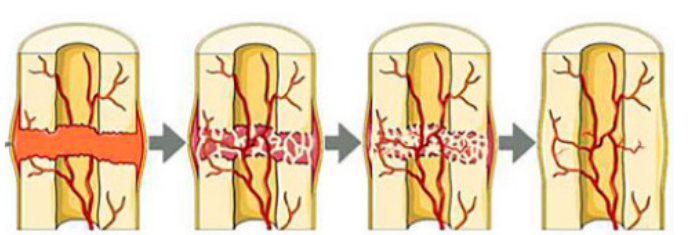


FIGURE 11. Schematic diagram of bioceramic derived for bone scaffold applications

Implantology of biodegradability bioceramic:



Mineralization and osteointegration due to ions release from bioceramic implant forming new bone tissue

FIGURE 12. Flow diagrams for biodegradability of bioceramic implant into new bone tissue regenerations

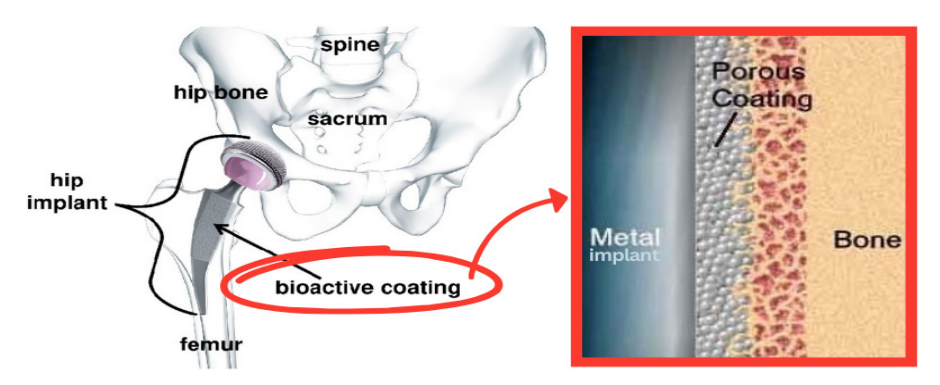


FIGURE 13. Detail diagram of bioceramic coating layer between the implant and bone tissue at heavy-load bearing applications

the scaffold is a sufficient amount of coating as its highest stress resistance up to 32 MPa with 46% porosity devoted as the preferable for adequate cell attachment. Next, research by Bakhsheshi-Rad et al. (2019) has studied the effect of akermanite coating associated with Poly-L-lactic acid (PLLA) and doxycycline (DOXY) on the magnesium alloy to enhance its biocompatibility, antibacterial activity and corrosion resistance. The slow degradation rate over a certain period improved the corrosion rate and elongated the duration of immersion of the Mg alloy with akermanitepolymer based coating. It has been recorded that the highest value of compressive strength was obtained after immersed in SBF solution for 7 days on the sample of Mg alloy with PLLA-AKT coated reaching 237 MPa compared to pure Mg alloy, PLLA coated and PLLA-AKT-DOXY coated devoted to an excellent mechanical strength exceeding the range of 100-230 MPa of human cortical bones. Meanwhile, the antibacterial activity and biocompatibility of the Mg alloy also has been improved due to the integration of DOXY that obstructs the intrusion of bacteria activity including S. aureus and E. coli.

Furthermore, besides the mechanical stability, the akermanite coating on the magnesium alloy, AZ91 is also capable of enhancing the corrosion resistance and cytocompatibility of the host tissue scaffold (Razavi et al. 2014a, 2014b). The magnesium is commonly known with low corrosion resistance that possibly caused the detaching of its particles from the bulk implant as well as fast degradation due to the reactions with the hydroxide ions and hydrogen gasses. Thus, the applied additive of akermanite coating on AZ91 has decelerated the corrosion rate after 4 weeks of immersion where the corrosion rate of AZ91 aided with akermanite coating slightly decreases 0.019 mg/cm²/h. Subsequently, it has improved the mechanical strength up to 45 MPa higher than uncoated AZ91 and cancellous bone which is within 2-12 MPa. Meanwhile, the findings on the cytocompatibility analysis by SEM imaging has certainly demonstrated the cell spreading in the akermanite coating samples reserved as the significant surface of cell growth compared to the uncoated AZ91. These appropriate results of AZ91

magnesium alloy assisted with nanostructured akermanite coating have promising the potentials of akermanite as the coating materials in bone implant applications.

CONCLUSION

Akermanite is one of the bioceramic materials that currently gained many attention among the researchers and deserved for a significant acknowledgement due to its outstanding performances that may be equal or exceed standard of other prominent bioceramic such as HA and β-TCP. Hence, this review discusses the production of akermanite that aims for alternative material for biomedical devices in the biomedical field specifically for bone tissue engineering applications. The further study on the properties and behaviours of akermanite such as mechanical strength and bioactivity performances were seen influenced by the processing method and applied parameters. According to multiple literatures by the previous studies, it can be concluded that the akermanite formation could be acquired by involving high sintering temperature at the range of 900-1350 °C. Consequently, the proper consideration in the ceramic production should be taken seriously for the purpose of producing great mineralogical properties on akermanite samples followed with providing adequate mechanical strength values within the range of human bone and positive biological performances with surrounding tissues. Comprehension on the mechanical strength of the akermanite should be clearly understood as it has a strong correlation with the physical properties incorporating the size particle, porosity and density of the samples since it impacts the mechanical bonding of the samples during the akermanite production. Meanwhile, the utilisation of akermanite also has demonstrated appropriate biological reactions by the formation of hydroxyapatite layer on the surface of the samples indicating the acceptance and compatibility between the implant material and the host tissue as well as given the opportunity of akermanite to be engaged in the biomedical device applications. This is because the rich contents of Ca, Mg, and Si substances in the akermanite samples has the crucial roles individually in the contribution of bone treatment and provide fast healing process as the proliferation rate and osteogenesis increases. Overall, the appropriate synthesis and processing methods, precursors and temperature parameters can achieve stable akermanite that has feasible potentials to be a promising and valuable bioceramic material for the biomedical devices applications. The favourable and controllable characteristics of akermanite bioceramic can be acquired through various methods of synthesis and various processing parameters applied in order to generate the desired properties suitable and can be beneficial in the bone tissue engineering practices.

ACKNOWLEDGMENTS

A gratitude was expressed to the Faculty of Mechanical Engineering & Technology and Faculty of Chemical Engineering & Technology of Universiti Malaysia Perlis (UniMAP) and School of Materials and Mineral Resources Engineering of Universiti Sains Malaysia (USM) for providing the equipment and facilities.

REFERENCES

- Arkame, Y., Harrati, A., Jannaoui, M., Et-Tayea, Y., Yamari, I., Sdiri, A. & Sadik, C. 2023. Effects of slag addition and sintering temperature on the technological properties of dolomite based porous ceramics. *Open Ceramics* 13: 100333. https://doi.org/10.1016/j.oceram.2023.100333
- Arokiasamy, P., Al Bakri Abdullah, M.M., Abd Rahim, S.Z., Luhar, S., Sandu, A.V., Jamil, N.H. & Nabiałek, M. 2022. Synthesis methods of hydroxyapatite from natural sources: A review. *Ceramics International* 48(11): 14959-14979. https://doi.org/10.1016/j.ceramint.2022.03.064
- Bakhsheshi-Rad, H.R., Akbari, M., Ismail, A.F., Aziz, M., Hadisi, Z., Pagan, E., Daroonparvar, M. & Chen, X. 2019. Coating biodegradable magnesium alloys with electrospun poly-l-lactic acid-åkermanite-doxycycline nanofibers for enhanced biocompatibility, antibacterial activity, and corrosion resistance. *Surface and Coatings Technology* 377: 124898. https://doi.org/10.1016/j. surfcoat.2019.124898
- Bernardo, E., Carlotti, J-F., Dias, P.M., Fiocco, L., Colombo, P., Treccani, L., Hess, U. & Rezwan, K. 2014. Novel akermanite-based bioceramics from preceramic polymers and oxide fillers. *Ceramics International* 40(1): 1029-1035. https://doi.org/10.1016/j.ceramint.2013.06.100
- Cai, W.K., Liu, J.H., Zhou, C.H., Keeling, J. & Glasmacher, U.A. 2021. Structure, genesis and resources efficiency of dolomite: New insights and remaining enigmas. *Chemical Geology* 573: 120191. https://doi.org/10.1016/j.chemgeo.2021.120191.

- Che Azurahanim Che Abdullah, Emmellie Laura Albert, Lau Gee Een, Mazni Abu Zarin & Mohd Zaki Mohd Yusoff. 2022. Effect of thermal treatment on physical properties of Malaysian dolomitic limestone. *Int. J. Electroactive Mater.* 10: 18-23.
- Choudhary, R., Koppala, S. & Swamiappan, S. 2015. Bioactivity studies of calcium magnesium silicate prepared from eggshell waste by sol-gel combustion synthesis. *Journal of Asian Ceramic Societies* 3(2): 173-177. https://doi.org/10.1016/j.jascer.2015.01.002
- Collin, M.S., Venkatraman, S.K., Sriramulu, M., Shanmugam, S., Drweesh, E.A., Elnagar, M.M., Mosa, E.S. & Sasikumar, S. 2021. Solution combustion synthesis of functional diopside, akermanite, and merwinite bioceramics: Excellent biomineralization, mechanical strength, and antibacterial ability. *Materials Today Communications* 27: 102365. https://doi.org/10.1016/j.mtcomm.2021.102365
- Dasan, A., Kraxner, J., Grigolato, L., Savio, G., Elsayed, H., Galusek, D. & Bernardo, E. 2022. 3D printing of hierarchically porous lattice structures based on åkermanite glass microspheres and reactive silicone binder. *Journal of Functional Biomaterials* 13(1): 8. https://doi.org/10.3390/jfb13010008
- Dasan, A., Talimian, A., Kraxner, J., Galusek, D., Elsayed, H. & Bernardo, E. 2021. Åkermanite glass microspheres: Preparation and perspectives of sintercrystallization. *International Journal of Applied Glass Science* 12: 551-561. https://doi.org/10.1111/ ijag.16115
- Dasan, A., Elsayed, H., Kraxner, J., Galusek, D., Colombo, P. & Bernardo, E. 2020. Engineering of silicone-based mixtures for the digital light processing of åkermanite scaffolds. *Journal of the European Ceramic Society* 40(7): 2566-2572. https://doi.org/10.1016/j.jeurceramsoc.2019.11.087
- Dasan, A., Elsayed, H., Kraxner, J., Galusek, D. & Bernardo, E. 2019. Hierarchically porous 3D-printed akermanite scaffolds from silicones and engineered fillers. *Journal of the European Ceramic Society* 39(14): 4445-4449. https://doi.org/10.1016/j.jeurceramsoc.2019.06.021
- Deng, Z.L., Pan, M.Z., Hua, S.B., Wu, J.M., Zhang, X.Y. & Shi, Y.S. 2023. Mechanical and degradation properties of triply periodic minimal surface (TPMS) hydroxyapatite & akermanite scaffolds with functional gradient structure. *Ceramics International* 49(12): 20808-20816. https://doi.org/10.1016/j.ceramint.2023.03.213
- Díaz-Pérez, M., Grima, L., Moshtaghioun, B.M. & Peña, J.I. 2021. CaO–MgO–SiO₂–P₂O₅- based multiphase bio-ceramics fabricated by directional solidification: Microstructure features and *in vitro* bioactivity studies. *Ceramics International* 47(12): 17041-17048. https://doi.org/10.1016/j. ceramint.2021.03.011

- Dobriţa, C.I., Bădănoiu, A.I., Voicu, G., Nicoară, A.I., Dumitru, S.M., Puşcaşu, M.E., Chiriac, Ş., Ene, R. & Iordache, F. 2023. Porous bioceramic scaffolds based on akermanite obtained by 3D printing for bone tissue engineering. *Ceramics International* 49(22): 35898-35906. https://doi.org/10.1016/j.ceramint.2023.08.270
- Dong, X., Heidari, A., Mansouri, A., Hao, W.S., Dehghani, M., Saber-Samandari, S., Toghraie, D. & Khandan, A. 2021. Investigation of the mechanical properties of a bony scaffold for comminuted distal radial fractures: Addition of akermanite nanoparticles and using a freeze-drying technique. *Journal of the Mechanical Behavior of Biomedical Materials* 121: 104643. https://doi.org/10.1016/j.jmbbm.2021.104643
- Duman, Ş. & Bulut, B. 2021. Effect of akermanite powders on mechanical properties and bioactivity of chitosan-based scaffolds produced by 3D-bioprinting. *Ceramics International* 47(10): 13912-13921. https://doi.org/10.1016/j.ceramint.2021.01.258
- Han, Z., Feng, P., Gao, C., Shen, Y., Shuai, C. & Peng, S. 2014. Microstructure, mechanical properties and *in vitro* bioactivity of akermanite scaffolds fabricated by laser sintering. *Bio-Medical Materials and Engineering* 24(6): 2073-2080. https://doi.org/10.3233/BME-141017
- Harrati, A., Arkame, Y., Manni, A., Aqdim, S., Zmemla, R., Chari, A., El Bouari, A., El Hassani, I-E.E.A., Sdiri, A., Hassani, F.O. & Sadik, C. 2022. Akermanitebased ceramics from Moroccan dolomite and perlite: Characterization and *in vitro* bioactivity assessment. *Open Ceramics* 10: 100276. https://doi. org/10.1016/j.oceram.2022.100276
- Hussin, K., Shamsul, J., Ruzaidi, C.M., Sobri, M.I., Nazry, M.S. & Nizar, K. 2006. The development of artificial marble from dolomite (Batu Reput). 2006 TMS Fall Extraction and Processing Division: Sohn International Symposium. pp. 617-621. https://doi. org/10.13140/2.1.1044.8325
- Li, X., Zhang, H. & Zhang, H. 2024. Fabrication of β-TCP/Akermanite composite scaffold via DLP and *in-situ* modification of micro-nano surface morphology for bone repair. *Ceramics International* 50(2, Part A): 2659-2669. https://doi.org/10.1016/j.ceramint.2023.10.276
- Liebschner, M.A.K. 2004. Biomechanical considerations of animal models used in tissue engineering of bone. *Biomaterials* 25(9): 1697-1714. https://doi.org/10.1016/S0142-9612(03)00515-5
- Liu, A., Sun, M., Yang, X., Ma, C., Liu, Y., Yang, X., Yan, S. & Gou, Z. 2016. Three-dimensional printing Akermanite porous scaffolds for load-bearing bone defect repair: An investigation of osteogenic capability and mechanical evolution. *Journal of Biomaterials Applications* 31(5): 650-660. https:// doi.org/10.1177/0885328216664839

- Liu, Q., Cen, L., Yin, S., Chen, L., Liu, G., Chang, J. & Cui, L. 2008. A comparative study of proliferation and osteogenic differentiation of adipose-derived stem cells on akermanite and β-TCP ceramics. *Biomaterials* 29(36): 4792-4799. https://doi.org/10.1016/j.biomaterials.2008.08.039
- Liu, W., Wang, T., Zhao, X., Dan, X., Lu, W.W. & Pan, H. 2016. Akermanite used as an alkaline biodegradable implants for the treatment of osteoporotic bone defect. *Bioactive Materials* 1(2): 151-159. https:// doi.org/10.1016/j.bioactmat.2016.11.004
- Ma, N., Ma, B., Zhou, Y., Zhu, H., Zhou, Y., Huan, Z., Wang, P. & Chang, J. 2019. *In vivo* evaluation of the subchronic systemic toxicity of akermanite bioceramic for bone regeneration following ISO standard methods. *RSC Advances* 9(31): 17530-17536. https://doi.org/10.1039/c9ra02496d
- Mohammadi, H., Baba Ismail, Y.M., Bin Shariff, K.A. & Mohd Noor, A.F. 2021a. Microstructure evolution, grain growth kinetics and mechanical properties of Ca₂MgSi₂O₇ bioceramics sintered at various temperatures. *Processing and Application of Ceramics* 15(4): 357-365. https://doi.org/10.2298/PAC2104357M
- Mohammadi, H., Sepantafar, M., Muhamad, N. & Sulong, A.B. 2021b. How does scaffold porosity conduct bone tissue regeneration? *Advanced Engineering Materials* 23(10): 2100463. https://doi.org/10.1002/adem.202100463
- Mohammadi, H., Baba Ismail, Y.M., Bin Shariff, K.A. & Mohd Noor, A.F. 2018. Synthesis and characterization of akermanite by mechanical milling and subsequent heat treatment. *Journal of Physics: Conference Series* 1082: 012021. https://doi.org/10.1088/1742-6596/1082/1/012021
- Myat-Htun, M., Mohammadi, H., Mohd Noor, A.F., Kawashita, M. & Baba Ismail, Y.M. 2021. Comprehensive investigation of phase formation mechanism and physico-mechanical properties of ca-Mg-silicate. *ASEAN Engineering Journal* 11(2): 37-50. https://doi.org/10.11113/AEJ.V11.16676
- Najafinezhad, A., Abdellahi, M., Ghayour, H., Soheily, A., Chami, A. & Khandan, A. 2017. A comparative study on the synthesis mechanism, bioactivity and mechanical properties of three silicate bioceramics. *Materials Science and Engineering C* 72: 259-267. https://doi.org/10.1016/j.msec.2016.11.084
- Nazry, M.S., Hafiz, F.K., Nizar, K.I., Ruzaidi, C.M., Saad, S.A. & Daud, S. 2006. Characterization and application of dolomite rock in Perlis. *Proceedings* of the 1st International Conference on Natural Resources Engineering & Technology, 24-25th July, Putrajaya, Malaysia, pp. 465-470.

- Putra, N.E., Leeflang, M.A., Klimopoulou, M., Dong, J., Taheri, P., Huan, Z., Fratila-Apachitei, L.E., Mol, J.M.C., Chang, J., Zhou, J. & Zadpoor, A.A. 2023.
 Extrusion-based 3D printing of biodegradable, osteogenic, paramagnetic, and porous FeMnakermanite bone substitutes. *Acta Biomaterialia* 162: 182-198. https://doi.org/10.1016/j.actbio.2023.03.033
- Razavi, M., Fathi, M., Savabi, O., Beni, B.H., Vashaee, D. & Tayebi, L. 2014a. Surface microstructure and *in vitro* analysis of nanostructured akermanite (Ca₂MgSi₂O₇) coating on biodegradable magnesium alloy for biomedical applications. *Colloids and Surfaces B: Biointerfaces* 117: 432-440. https://doi.org/10.1016/j.colsurfb.2013.12.011
- Razavi, M., Fathi, M., Savabi, O., Mohammad Razavi, S., Beni, B.H., Vashaee, D. & Tayebi, L. 2014b. Controlling the degradation rate of bioactive magnesium implants by electrophoretic deposition of akermanite coating. *Ceramics International* 40(3): 3865-3872. https://doi.org/10.1016/j.ceramint.2013.08.027
- Ren, Q., Ren, Y., Wu, X., Bai, W., Zheng, J. & Hai, O. 2019. Effects of pyrolusite and dolomite co-additives on the structure and properties of bauxite-based ceramics. *Materials Chemistry and Physics* 230: 207-214. https://doi.org/10.1016/j.matchemphys.2019.03.072
- Shahraki, B.K., Mehrabi, B. & Dabiri, R. 2009. Thermal behavior of Zefreh dolomite mine (Centeral Iran). *Journal of Mining and Metallurgy, Section B: Metallurgy* 45B(1): 35-44. https://doi.org/10.2298/JMMB0901035S
- Sharafabadi, A.K., Abdellahi, M., Kazemi, A., Khandan, A. & Ozada, N. 2017. A novel and economical route for synthesizing akermanite (Ca₂MgSi₂O₇) nanobioceramic. *Materials Science and Engineering C* 71: 1072-1078. https://doi.org/10.1016/j.msec.2016.11.021
- Sharma, S. 2022. Significant contribution of deeper traps for long afterglow process in synthesized thermoluminescence material. *Journal of Mineral and Material Science (JMMS)* 3(4): 1049. https://doi.org/10.54026/jmms/1049
- Tavangarian, F., Zolko, C.A. & Davami, K. 2021. Synthesis, characterization and formation mechanisms of nanocrystalline akermanite powder. *Journal of Materials Research and Technology* 11: 792-800. https://doi.org/10.1016/j.jmrt.2021.01.021
- Tavangarian, F., Zolko, C.A., Sadeghzade, S., Fayed, M. & Davami, K. 2020. Fabrication, mechanical properties and *in-vitro* behavior of akermanite bioceramic. *Materials* 13(21): 4887. https://doi.org/10.3390/ma13214887

- Tengku Mustafa, T.N.A.S., Munusamy, S.R.R., Uy Lan, D.N. & Yunos, N.F.M. 2016. Physical and structural transformations of Perlis carbonate rocks via mechanical activation route. *Procedia Chemistry* 19: 673-680. https://doi.org/10.1016/j.proche.2016.03.069
- Tursunov, O., Dobrowolski, J. & Nowak, W. 2015. Catalytic energy production from municipal solid waste biomass: Case study in Perlis-Malaysia. *World Journal of Environmental Engineering* 3(1): 7-14. https://doi.org/10.12691/wjee-3-1-2
- Wu, C. & Chang, J. 2004. Synthesis and apatite-formation ability of akermanite. *Materials Letters* 58(9): 2415-2417. https://doi.org/10.1016/j.matlet.2004.02.039
- Yamamoto, O., Ohira, T., Mohan, D.J., Fukuda, M., Özkal, B., Sawai, J. & Nakagawa, Z-e. 2008. Antibacterial characteristics of carboncoated CaCO₃/Mg0 powder led by the pyrolysis of poly (vinyl alcohol)-dolomite mixture. *TANSO* 2008(232): 77-81. https://doi.org/10.7209/tanso.2008.77
- Yang, H., Hazen, R.M., Downs, R.T. & Finger, L.W. 1997. Structural change associated with the incommensurate-normal phase transition in akermanite, Ca₂MgSi₂O₇, at high pressure. *Physics and Chemistry of Minerals* 24(7): 510-519. https://doi.org/10.1007/s002690050066
- Youness, R.A., Zawrah, M.F. & Taha, M.A. 2024. Fabrication of akermanite scaffolds with high bioactivity and mechanical properties suitable for bone tissue engineering application. *Ceramics International* 50(18 Part A): 32253-32264. https://doi.org/10.1016/j.ceramint.2024.06.033
- Yue, X., Jiao, X., Xu, C., Zhang, Y., Wu, F., Wang, H., Zhu, Q., Zhang, Z., Zhao, L., Sun, X., Yang, X., He, F., Gou, Z., Yang, G. & Zhang, L. 2024. 3D printing novel porous granule-type bioceramics via magnesium tuning biological performances beneficial for implantation and clinical translation. *Chemical Engineering Journal* 486: 150401. https:// doi.org/10.1016/j.cej.2024.150401
- Zadehnajar, P., Mirmusavi, M.H., Soleymani Eil Bakhtiari, S., Bakhsheshi-Rad, H.R., Karbasi, S., RamaKrishna, S. & Berto, F. 2021. Recent advances on akermanite calcium-silicate ceramic for biomedical applications. *International Journal of Applied Ceramic Technology* 18(6): 1901-1920. https://doi.org/10.1111/jjac.13814
- Zhang, M., Yang, N., Dehghan-Manshadi, A., Venezuela, J., Bermingham, M.J. & Dargusch, M.S. 2023. Fabrication and properties of biodegradable akermanite-reinforced Fe35Mn alloys for temporary orthopedic implant applications. ACS Biomaterials Science and Engineering 9(3): 1261-1273. https://doi.org/10.1021/acsbiomaterials.2c01228

^{*}Corresponding author; email: hasnidahnur@gmail.com